

## THE KINETICS OF THE INTERACTIONS OF O<sub>2</sub> AND N<sub>2</sub>O WITH A Cu(110) SURFACE AND OF THE REACTION OF CO WITH ADSORBED OXYGEN STUDIED BY MEANS OF ELLIPSOMETRY, AES AND LEED

F.H.P.M. HABRAKEN and G.A. BOOTSMA

*Van 't Hoff Laboratory, University of Utrecht, Padualaan 8, 3584 CH Utrecht, The Netherlands*

Received 23 March 1979; manuscript received in final form 31 May 1979

Ellipsometry, LEED and Auger electron spectroscopy have been used to study the interactions of O<sub>2</sub> and N<sub>2</sub>O with a clean annealed Cu(110) surface and the reaction of CO with adsorbed oxygen in the monolayer range. Gas pressures were in the range 10<sup>-8</sup>–10<sup>-4</sup> Torr and crystal temperatures varied between 23–400°C. The changes in the ellipsometric angles  $\Delta$  and  $\psi$  per oxygen atom upon adsorption and removal of oxygen depend on the coverage  $\theta$ , the temperature and on the azimuth of the plane of incidence of the light beam. The kinetics of the chemisorption of oxygen is independent of the crystal temperature, initial sticking probability  $\approx 0.2$ . The LEED data and the adsorption kinetics indicate an attractive interaction in the adsorbed layer in the [001] direction. The initial decomposition probability of N<sub>2</sub>O at room temperature is 0.15 and decreases with increasing temperature; the maximum coverage is 0.5 monolayer. The LEED patterns observed were the same as those with O<sub>2</sub>. The reaction probability of CO with adsorbed oxygen increases with decreasing oxygen coverage (order of magnitude  $\sim 10^{-5}$ , apparent activation energy  $\sim 6$  kcal/mol). This increase has been attributed to the operation of the Langmuir–Hinshelwood mechanism.

### 1. Introduction

The adsorption of molecular oxygen on Cu(110) has been investigated with LEED [1–4], work function measurements [5,6], AES [5,7] and low energy ion scattering [8]. The results suggest that at room temperature the initial sticking probability  $s(0) \approx 0.05$ –0.1. Initially LEED patterns showed streaks parallel to the reciprocal [110] direction, changing into a (2 × 1) pattern after an exposure of 60–600 L (1 L = 10<sup>-6</sup> Torr s = 1.33 × 10<sup>-4</sup> Pa s) [1–4]. Further exposure at room temperature caused an increase in the background intensity and the appearance of weak spots of a c(6 × 2) structure; this pattern was more easily obtained at higher temperatures [1,2]. Other patterns have been observed after exposures at crystal temperatures of about 400°C [3,4].

Ertl and Küppers [5] have found an increase in the work function  $\Delta\phi = 0.2$  eV after an exposure of 6 L O<sub>2</sub> to Cu(110). Delchar [6] reported a maximum increase  $\Delta\phi = 0.7$  eV after an oxygen exposure of 2 × 10<sup>3</sup> L.

From low energy ion scattering experiments it has been concluded that upon exposures of  $\sim 10^{-6}$  Torr min no surface reconstruction takes place and that the adsorbed oxygen atoms are located  $0.6 \pm 0.1$  Å below the midpoint between two neighbouring Cu atoms in a [001] direction [8].

Ellipsometric results obtained at atmospheric pressure and at temperatures from 70 to 178°C showed rapid oxidation of Cu(110) within the range of oxide thicknesses 10–100 Å, but no data in the submonolayer range have been reported [9].

On copper surfaces nitrous oxide decomposes into desorbing N<sub>2</sub> and a chemisorbed oxygen atom [1,10]. According to Ertl [1] streak formation in the LEED pattern takes place after an exposure of 6 L N<sub>2</sub>O to Cu(110) and a sharp ( $2 \times 1$ ) pattern is observed only after exposures of 60 L at higher temperatures (300°C).

The reaction of CO with oxygen adsorbed on Cu(110) has been investigated with LEED by Ertl [11]. By measuring the intensity of spots of the  $c(6 \times 2)$  and  $(2 \times 1)$  superstructures as a function of CO exposure, he obtained an activation energy of 5 kcal/mol.

In a previous paper we presented the results of an ellipsometry–AES–LEED study of the kinetics of the interactions of O<sub>2</sub> and N<sub>2</sub>O with a Cu(111) surface and of the reaction of CO with adsorbed oxygen [12]. In this paper we report on the same reactions on a clean annealed Cu(110) surface.

The results are confined to the monolayer range. A preliminary account of the interaction of O<sub>2</sub> with Cu(110) has been given in ref. [13]. In a companion paper subsequent stages of initial oxidation as revealed by the combination of work function measurements, ellipsometry, AES and LEED are described [14]. For the chemisorption stage of N<sub>2</sub>O and O<sub>2</sub> the present results show an apparent plane-specificity with higher rates for Cu(110) than for Cu(111), in contrast with the apparent non-plane-specific behaviour of the CO oxidation reaction.

## 2. Experimental

The experimental arrangement and procedures were essentially the same as described in ref. [12]. A disc-shaped crystal, spark-cut from a 5N copper rod (Material Research Corporation) to within 2° of the (110) orientation, was ground, electro-lap polished and mounted in the crystal holder. The surface was cleaned by applying cycles of sputtering (600 V, 5 μA/cm<sup>2</sup>, 10<sup>-4</sup> Torr Ar) and annealing (450°C). Auger spectra showed that the amount of any contaminant on the surface was less than about 3% of a monolayer.

The changes in the ellipsometric angles  $\delta\Delta (\equiv \bar{\Delta} - \Delta)$  and  $\delta\psi (\equiv \bar{\psi} - \psi; \bar{\Delta}, \bar{\psi}$  clean surface) were determined with off-null irradiance measurements (during continuous exposures) or by two-zone measurements (interrupted exposures). The wavelength was 632.8 nm and the angle of incidence  $69 \pm 1^\circ$ . The azimuth  $\Omega$ , defined as the angle between the plane of incidence of the light beam and the rows on the surface ([ $\bar{1}10$ ] direction) was varied.

The Auger spectra were recorded with a four-grid retarding field analyser. The current of the primary beam was  $40\ \mu\text{A}$ , its energy 2500 eV and the angle of incidence about  $8^\circ$  with the surface. The modulation voltage on the retarding grids was 10 V p-p. As a measure for the oxygen coverage the ratio  $h_O/h_{Cu}$  of the oxygen 510 eV and the copper 920 eV peak-to-peak heights in the second derivative spectra were taken.

For the CO exposures high purity carbon monoxide (L'Air Liquide, 99.997 vol %) was used. During all exposures the gas was continuously renewed by pumping with the turbomolecular pump.

### 3. Ellipsometric results and calibration

#### 3.1. Anisotropy

It appeared that the change in  $\Delta$  per adsorbed oxygen atom was a function of the coverage  $\theta$ , the crystal temperature  $T$  and the azimuth  $\Omega$ , while  $\delta\psi$  per O atom turned out to be only a function of  $\Omega$ . This is in contrast with the observations on the Cu(111) plane [12]. In fig. 1,  $\delta\Delta$  is depicted versus the oxygen Auger signal at different  $T$  for  $\Omega = 90^\circ$ . At room temperature a linear relationship was observed between the oxygen Auger signal and  $\delta\Delta$ . Then  $\delta\psi \approx 0.25\ \delta\Delta$ . The same curves result from the interaction of  $N_2O$  with Cu(110) as well as from the removal of

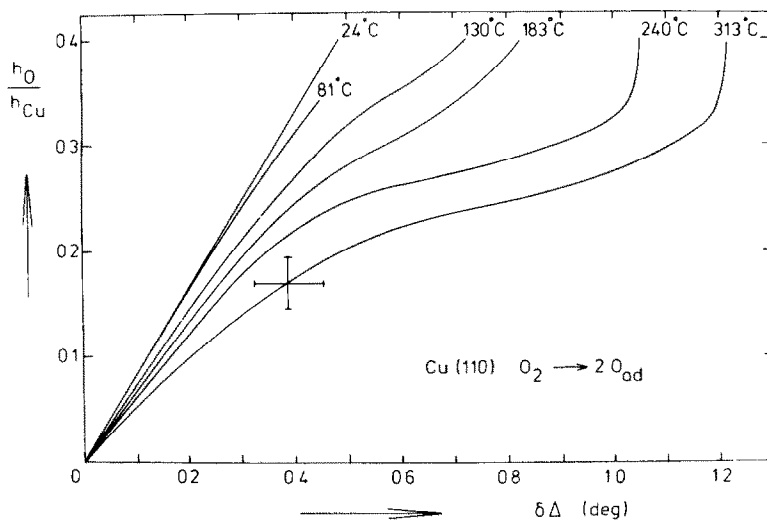


Fig. 1. Ratio of the O 510 eV to the Cu 920 eV Auger peak versus  $\delta\Delta$  upon adsorption of oxygen on Cu(110) at different temperatures ( $\Omega = 90^\circ$ ).  $T = 24, 240$  and  $313^\circ\text{C}$ ; two-zone measurements.  $T = 81, 130$  and  $183^\circ\text{C}$ : off-null irradiance measurements. Bars: estimated errors.

adsorbed oxygen with CO. An adsorption experiment at 313°C delivered a total  $\delta\Delta$  of about 1.2° and a subsequent reduction of the surface with CO at 183°C yielded a total  $\delta\Delta$  of about 0.8°. This indicates that the curves of fig. 1 are reversible with respect to  $T$ .

For  $\Omega = 0^\circ$  (plane of incidence parallel to the troughs) the curve of fig. 1 at  $T = 24^\circ\text{C}$  was observed at all temperatures considered. In this case the maximum  $\delta\psi$  was 0.29°. For  $\Omega \approx 45^\circ$  intermediate curves were observed, then  $\delta\psi$  amounted to 0.17°.

It must be concluded that the larger  $\delta\Delta$  at the same  $h_{\text{O}}/h_{\text{Cu}}$  at higher temperatures is not due to a larger uptake of oxygen. Most probably this effect is caused by a temperature dependent, anisotropic bonding of the oxygen atoms to the substrate. Optical anisotropy has been observed with ellipsometry in oxide films (thickness 100–1200 Å) on copper single crystals with surfaces of (110) and (311) orientation [15]. The observed anisotropy will be discussed in a forthcoming paper [16].

### 3.2. Calibration

At room temperature the slopes in the  $h_{\text{O}}/h_{\text{Cu}}$  versus  $\delta\Delta$  plots for Cu(110) and Cu(111) [12] are the same within experimental accuracy ( $\pm 10\%$ ) (fig. 2). The absolute heights of the Cu LMM Auger peaks are equal for the clean surfaces of both planes; the attenuation at the highest coverage in the chemisorption stage was  $\leq 10\%$ . Thus for  $T = 23^\circ\text{C}$  and at higher  $T$ , when  $\Omega = 0^\circ$ , the  $\delta\Delta$  per adsorbed atom is the same for Cu(110) and Cu(111).

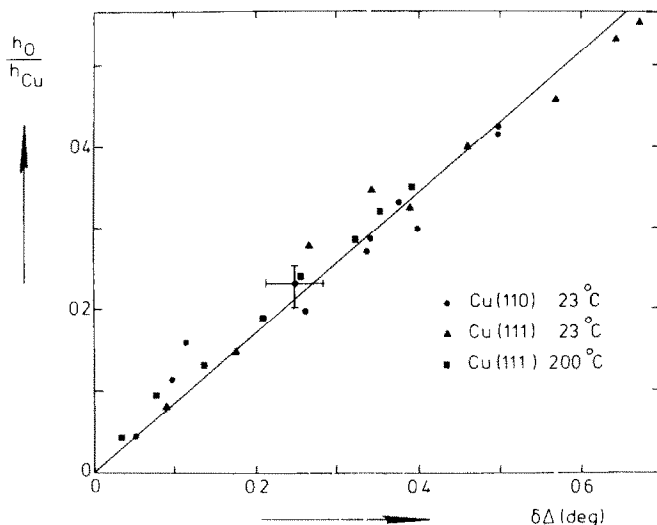


Fig. 2. Oxygen Auger signal versus  $\delta\Delta$  upon oxygen adsorption on Cu(111) ( $23^\circ\text{C}$ ) and on Cu(110) ( $23^\circ\text{C}$ ) and upon removal of oxygen from Cu(111) ( $T = 200^\circ\text{C}$ ).

The  $(2 \times 1)$  LEED pattern at the saturation point of the chemisorption stage permits an absolute calibration of the coverage. Assuming that no reconstruction takes place during exposures in the  $10^{-6}$  Torr min range [8] we conclude that the  $(2 \times 1)$  pattern corresponds to  $\theta = 0.5$ . Thus for the chemisorption stage on Cu(110)

$$\theta = (1.25 \pm 0.15) \times h_O/h_{Cu} \quad (1a)$$

for  $h_O/h_{Cu} \leq 0.40$ , and at  $\Omega = 0^\circ$

$$\theta = (1.0 \pm 0.1) \times \delta\Delta \quad (1b)$$

for  $\delta\Delta \leq 0.49^\circ$ . For  $\theta > 0.5$  incorporation of oxygen is assumed to occur [14], as on Cu(100) [17].

#### 4. Interaction of $O_2$ and $N_2O$ with Cu(110)

##### 4.1. Adsorption of oxygen

Oxygen was exposed to a Cu(110) surface in the pressure range  $10^{-8}$ – $10^{-4}$  Torr and at crystal temperatures between 23 and  $360^\circ\text{C}$ . In fig. 3 an example of  $\delta\Delta$  as a function of time of exposure at room temperature is shown. When the changes in  $\Delta$  became too small to be measured, the pressure was increased.

Fig. 4 shows the oxygen Auger signal as a function of  $O_2$  exposure at different

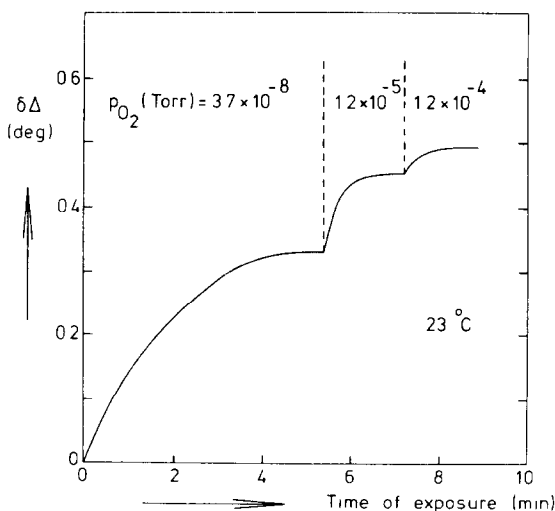


Fig. 3.  $\delta\Delta$  (off-null irradiance measurements) versus time, during exposure of oxygen to Cu(110) at increasing pressures.

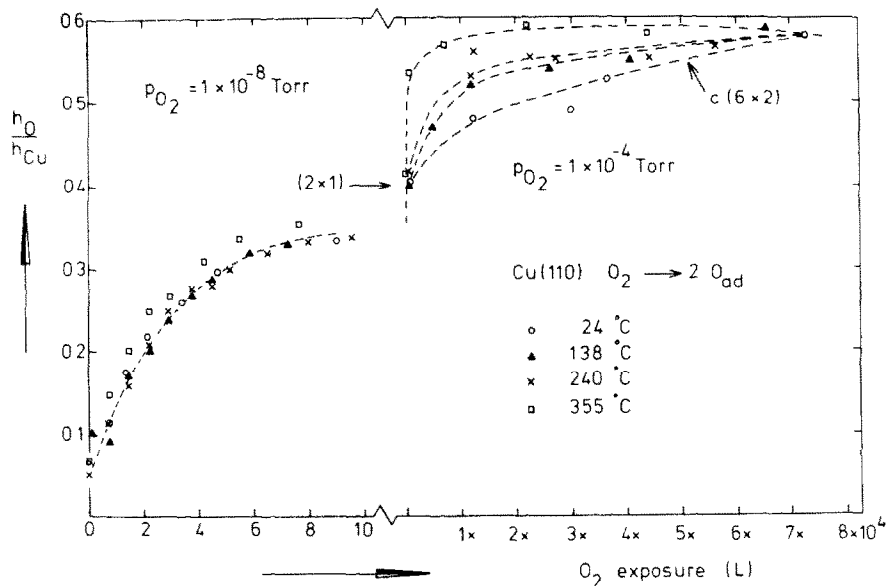


Fig. 4. Oxygen Auger signal as a function of exposure of O<sub>2</sub> to Cu(110) at different temperatures.

crystal temperatures. Starting with a surface totally free of oxygen turned out to be difficult (as revealed by AES). The reason for this may have been the adsorption or segregation of oxygen during annealing and cooling after sputtering or during the recording of an Auger spectrum.

At the start of an exposure a pressure of  $10^{-8}$  Torr was taken. After 10 L the pressure was increased to  $10^{-7}$  Torr until  $h_O/h_{Cu} = 0.40$ . Further exposures were made in the  $10^{-4}$  Torr range. The Auger spectra were recorded after evacuation down to  $5 \times 10^{-10}$  Torr in the low exposure region and to about  $5 \times 10^{-9}$  Torr in the high exposure region. No influence of the ionisation pressure gauge was observed.

After a few Langmuirs streaks appeared in the LEED pattern in the reciprocal  $[\bar{1}10]$  direction. These streaks condensed into spots and a  $(2 \times 1)$  pattern developed. This was at its sharpest around 360 L with  $h_O/h_{Cu} = 0.40$ . At larger exposures the  $c(6 \times 2)$  superstructure was observed via an increase in the background intensity and the formation of a domain structure as has been reported earlier [1].

#### 4.2. Decomposition of nitrous oxide

In contrast to Cu(111) [12], on the Cu(110) plane N<sub>2</sub>O appeared to have a large reaction probability. So the exposures were initially performed at N<sub>2</sub>O pressures of  $10^{-7}$  Torr, and at higher  $\theta$  with  $10^{-5}$  Torr. Further procedures were essentially the

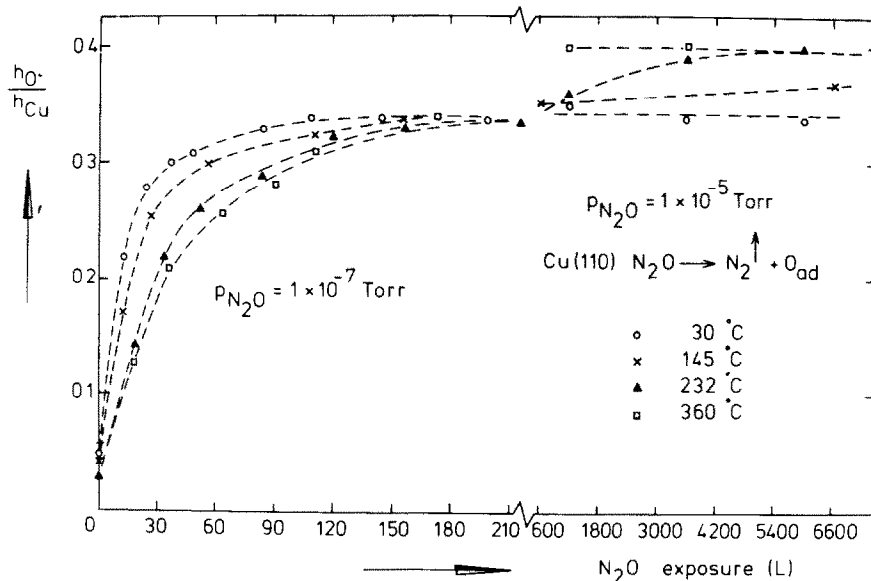


Fig. 5. Oxygen Auger signal as a function of exposure of  $N_2O$  to Cu(110) at different temperatures.

same as they had been with the  $O_2$  adsorption experiments, except for the fact that in these experiments the hot filament of the ionisation gauge was switched off during the exposures to prevent formation of NO species [12].

In fig. 5 the oxygen Auger signal is depicted as a function of the  $N_2O$  exposure at different temperatures. No nitrogen has been found in the Auger spectra. At all  $T$  ( $<400^\circ\text{C}$ ) the maximum  $h_O/h_{Cu} \approx 0.40$ , up to exposures of  $10^5$  L. The LEED patterns observed were the same as those with  $O_2$ . From fig. 5 it follows that the reaction rate decreases with increasing  $T$  for  $h_O/h_{Cu} \leq 0.34$ . Above this coverage, the reverse is the case.

#### 4.3. Discussion of the $O_2$ adsorption

In fig. 6 a plot is shown of the sticking probability as a function of the oxygen coverage at room temperature. The initial sticking probability is about 0.17. This value compares reasonably well with values derived from the literature [1,2,7].  $O_2$  reacts more easily with Cu(110) than with Cu(111) ( $s(0) \approx 10^{-3}$  [12]) and Ag(110) ( $s(0) = 5 \times 10^{-4}$  [18]). The initial reactivity of polycrystalline copper films ( $s(0) \approx 0.1$  [19]) compares with that of Cu(110).

Fig. 6 shows that the adsorption rate is proportional to the pressure for all  $\theta$ . The results obtained with  $N_2O$  and for the reduction with CO (section 5) strongly indicate that  $O_2$  chemisorbs dissociatively on Cu(110). The occurrence of the

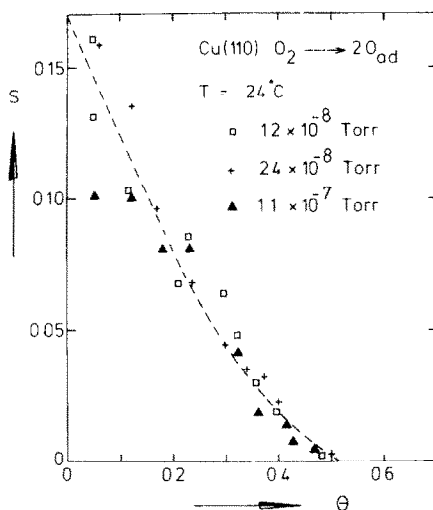


Fig. 6. Oxygen sticking coefficient  $s$  versus  $\theta$ , derived from continuous ellipsometric measurements at room temperature. The dashed line represents eq. (4) with  $\omega' = 0$  kcal/mol and  $\omega'' = 4$  kcal/mol.

ordered ( $2 \times 1$ ) pattern, while no restructuring of the Cu surface takes place [8], points to lateral interactions in the adsorbed layer.

When two empty adjacent sites are necessary for dissociation, then the lateral interactions have to be taken into account in the model for the kinetics. This can be achieved by the introduction of the parameter  $\theta_{00}$ , which is the probability that two nearest neighbour (nn) adsorption sites are empty at a given  $\theta$  (cf. refs. [20,21]). In this case  $\theta_{00}$  has to be calculated for the rectangular lattice of the Cu(110) plane, with two different pair-wise interaction energies,  $\omega'$  and  $\omega''$  for the  $[\bar{1}10]$  and the  $[001]$  direction, respectively. If thermodynamic equilibrium is assumed and only nn interactions are taken into account, then one gets for a one-dimensional chain of sites [20]:

$$N'_{00} = N'_s \left( 1 - \theta - \frac{2\theta(1-\theta)}{\{1 - 4\theta(1-\theta)(1 - e^{\omega'/RT})\}^{1/2} + 1} \right), \quad \theta'_{00} = N'_{00}/N'_s. \quad (2)$$

Here  $\omega'$  is the pair-wise interaction energy ( $\omega'$  is negative for repulsive and positive for attractive interactions),  $\theta$  the coverage ( $\equiv N'_1/N'_s$ ,  $N'_{00}$  the number of empty nn site pairs,  $N'_s$  the number of adsorption sites and  $N'_1$  the number of occupied sites, all per unit length. The parameter  $\theta_{00}$  for a (110) plane can then be evaluated by adding  $N'_{00}$  and  $N''_{00}$  for the two directions  $[\bar{1}10]$  and  $[001]$ :

$$N_{00} = N'_{00}N''_s + N''_{00}N'_s,$$

and

$$\theta_{00} = \frac{N_{00}}{2N_s} = \frac{N'_{00}N''_s + N''_{00}N'_s}{2N'_sN''_s} = \frac{1}{2}(\theta'_{00} + \theta''_{00}). \quad (3)$$

Here  $N_{00}$  and  $N_s$  are defined per unit of surface area. In this so-called quasi-chemical approximation it has been assumed, that pairs of nn sites in two different directions may be treated as being independent of each other, although in fact they are not [20]. (A more detailed evaluation of the two-dimensional case has been attempted by De Wit [22].) Finally one obtains from eqs. (2) and (3)

$$\theta_{00} = 1 - \theta - \theta(1 - \theta) \left[ \{ (1 - 4\theta(1 - \theta)(1 - e^{\omega'/RT}))^{1/2} + 1 \}^{-1} + \{ (1 - 4\theta(1 - \theta)(1 - e^{\omega''/RT}))^{1/2} + 1 \}^{-1} \right]. \quad (4)$$

For  $\omega' = \omega''$ , eq. (4) reduces to the result obtained by Hill [20] and King and Wells [21] for a lattice with four-fold symmetry.

It appears that the measured sticking probability  $s(\theta)$  (fig. 6) can be described by

$$s(\theta) = s(0) \theta_{00}, \quad (5)$$

with  $s(0) \approx 0.17$ . Two parameters in eq. (5), namely  $\omega'$  and  $\omega''$ , may be adjusted to obtain a good fit to the data of fig. 6. Streak formation in the LEED pattern at low coverages indicates order in the [001] and disorder in the  $[\bar{1}10]$  direction. This is very probably the result of strong attractive interactions between the adatoms (possibly via the substrate) in the [001] direction and weak interactions in the  $[\bar{1}10]$  direction. Consistent with this conclusion, the data of fig. 6 can be explained with eqs. (4) and (5) if  $\omega'$  is taken between  $-1$  and  $1$  kcal/mol and  $\omega'' \geq 4$  kcal/mol. It has been assumed that the surface consists of specific sites of two nn copper surface atoms in the  $[\bar{1}10]$  direction. The combined data (fig. 4, cf. also ref. [14]) show that the completed  $(2 \times 1)$  structure represents the maximum coverage for the chemisorption stage and therefore the relative coverage  $\theta' = \theta/\theta_{\text{sat}}$  is used instead of  $\theta$  in fitting eq. (5) with the data of fig. 6.

Eq. (5) can be obtained in two ways. Firstly one can assume Langmuir kinetics, in which physisorbed oxygen molecules are supposed to have a negligible effect on the chemisorption kinetics and a gas molecule has a probability  $s(0)$  for chemisorption only when impinging on an empty nn site pair.

Secondly one can assume precursor state kinetics. In that case an expression for the sticking probability is [21]:

$$s(\theta') = s(0) [1 + K(\theta_{00}^{-1} - 1)]^{-1}. \quad (6)$$

Here  $s(0)$  and  $K$  are related to the condensation coefficient  $\alpha$  of gas molecules and to the probabilities for chemisorption ( $P_a$ ) and for desorption of the precursor molecules from an empty chemisorption nn site pair ( $P_d$ ) and from a nn site pair not available for chemisorption ( $P'_d$ ).  $K$  and  $s(0)$  are expressed as follows:

$$K = P'_d/(P_a + P_d), \quad s(0) = \alpha P_a/(P_a + P_d). \quad (7)$$

Eq. (5) is obtained when  $K = 1$ . The precursor state model has been used to describe the kinetics of the dissociative chemisorption of O<sub>2</sub> on Cu(111) [12]. On that plane the sticking probability was found to be initially independent of the coverage, but to depend on the crystal temperature. In the O<sub>2</sub>/Cu(110) system, however, the kinetics of chemisorption is independent of the crystal temperature within experimental accuracy (fig. 4), and the sticking probability decreases strongly with increasing oxygen coverage (fig. 6). This makes a description in terms of a precursor model less favourable.

There is a remarkable difference between the two copper planes (111) and (110) both with respect to the absolute value of  $s(0)$  as well as with respect to the  $\theta$  and  $T$  dependence. When oxygen is in the gas phase, mobile physisorbed O<sub>2</sub> molecules are expected to be present on both planes. On Cu(110) incident O<sub>2</sub> molecules, which undergo a direct transition into the chemisorbed state, may make a substantially larger contribution to the chemisorption rate than physisorbed O<sub>2</sub> molecules; on Cu(111) the reverse seems to be the case.

#### 4.4. Discussion of the N<sub>2</sub>O decomposition

In fig. 7 the reaction probability  $s$  of N<sub>2</sub>O at room temperature is depicted as a function of  $\theta$ . The reaction probability is defined as the number of oxygen atoms deposited per incident N<sub>2</sub>O molecule. The initial value  $s(0)$  is 0.15, which is much larger than on Cu(111) (extrapolated value at 30°C:  $\sim 10^{-9}$  [12]). The probability

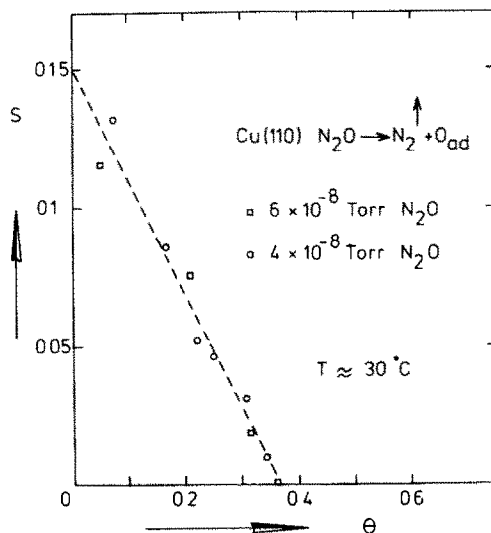


Fig. 7. Nitrous oxide reaction probability as a function of  $\theta$ , derived from continuous ellipsometric measurements at room temperature.

decreases linearly up to  $\theta = 0.36$  and then becomes very small. The coverage  $\theta = 0.5$  is reached after about  $10^5$  L. These results are in qualitative agreement with those which Ertl obtained using LEED [1].

The initial reaction probability decreases slightly with increasing crystal temperature (fig. 5). Values of  $s(0)$  derived from the Auger measurements are: 0.15 ( $30^\circ\text{C}$ ), 0.062 ( $145^\circ\text{C}$ ), 0.035 ( $232^\circ\text{C}$ ), 0.031 ( $330^\circ\text{C}$ ) and 0.022 ( $360^\circ\text{C}$ ). For the slope of an Arrhenius plot of  $s(0)$  a value of about 2 kcal/mol is calculated (pre-exponential factor  $6 \times 10^{-3}$ ), instead of  $-10.4$  kcal/mol for Cu(111) [12]. This dependence of  $s(0)$  on  $T$  points to the existence of a precursor prior to the transition to the final chemisorption state. Though the linear decrease of  $s$  with coverage (fig. 7) seems to favour a model without any precursor state, it can also be explained with a precursor state model.

It has been suggested [23,24] that the dissociation proceeds via the capture by  $N_2O$  of an electron from the substrate. The activation energy required to capture an electron will be associated with the work function. The work function difference between Cu(111) and Cu(110) (11 [25] to 14 kcal/mol [6]) equals approximately the difference between the activation energies for the  $N_2O$  decomposition on both planes (12.4 kcal/mol).

From fig. 5 it follows that the apparent activation energy for the decomposition increases with the oxygen coverage, and is zero for  $\theta \approx 1/3$ . This increasing apparent activation energy may be due to the increase in work function that results from oxygen adsorption [5,6,14]. According to section 4.3 the arrangement of the adsorbed atoms on the surface is rather independent of the temperature.

## 5. The oxidation of CO by preadsorbed oxygen

The reaction of adsorbed oxygen with carbon monoxide was studied in the temperature range  $230\text{--}410^\circ\text{C}$  and at CO pressures between  $5 \times 10^{-5}\text{--}5 \times 10^{-4}$  Torr. During the exposures of CO the ionisation gauge was switched off. The ratio of the partial pressures of CO and  $O_2$ , as determined with the mass spectrometer, turned out to be about  $5 \times 10^5$ .

The exposures were started at an oxygen coverage of 0.5 ( $(2 \times 1)$  pattern). In fig. 8,  $\delta\Delta$  (measured at  $\Omega = 0^\circ$ ) is depicted as a function of CO exposure at different temperatures ( $\theta \approx \delta\Delta$  (deg), eq. (1b)). A small amount of oxygen was generally still present after a reduction experiment, as monitored with AES (cf. section 4.1). No difference in the curves was observed between surface oxygen originating from  $O_2$  and  $N_2O$ .

The reaction rate appears to increase with decreasing oxygen coverage. In the whole coverage range this rate appears to be proportional to the CO pressure. An analogous increase in the reaction probability with decreasing oxygen coverage has been observed for the reaction of CO with oxygen adsorbed on Ag(110) [18,26,27].

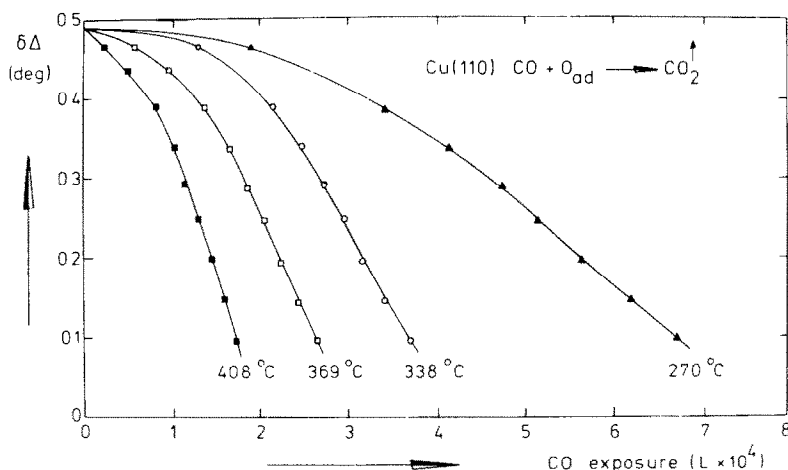


Fig. 8.  $\Delta\Delta$  versus exposure of CO to a surface with preadsorbed oxygen at different temperatures. Solid lines: ellipsometric off-null measurements ( $\Omega = 0^\circ$ ). Dots: integral of eq. (9) with ( $\blacktriangle$ )  $k_1 = 4.4 \times 10^{-5} \text{ L}^{-1}$ ; ( $\circ$ )  $k_1 = 8.5 \times 10^{-5} \text{ L}^{-1}$ ; ( $\square$ )  $k_1 = 9.8 \times 10^{-5} \text{ L}^{-1}$ ; ( $\blacksquare$ )  $k_1 = 1.34 \times 10^{-4} \text{ L}^{-1}$ ;  $k_2 = 2k_1$ ,  $\omega = 4 \text{ kcal/mol}$ .

In ref. [18] a one-dimensional model has been devised for a row of adsorbed atoms in the [001] direction with attractive interactions. In this model different rate constants were assumed for "lone" oxygen atoms and "row" oxygen atoms. A better adaptation is obtained, when this model includes the assumption that the reaction proceeds via the Langmuir–Hinshelwood (L–H) mechanism. Recently it has been shown that this is the path via which the oxidation of CO on Pd(111) (molecular beam study) [28] and polycrystalline Pt (isotope tracer method) [29] proceeds.

Let  $N_{11}$  be the number of occupied site pairs,  $N_{01}$  the number of pairs of sites that are occupied by one atom,  $N_1$  the total number of adsorbed atoms and  $N_s$  the total number of sites. Then the rate equation becomes:

$$dN_1/d(pt) = (-k_2 N_{01} - 2k_1 N_{11})(N_s - N_1)/N_s, \quad (8)$$

with different rate constants  $k_2$  and  $k_1$  for different types of oxygen (cf. eq. (7) of ref. [18]). The factor  $(N_s - N_1)/N_s$  has been included to take account of the L–H mechanism and it denotes the probability that a site in a neighbouring [001] row is empty and available for CO molecules. In the experimental conditions only a very small quantity of CO is adsorbed (heat of adsorption  $\approx 13.1 \text{ kcal/mol}$  [30]). We assume that this quantity is proportional to the CO pressure, justifying the use of the product of pressure and time in the left hand side of eq. (8). Finally we get:

$$\frac{d\theta'}{d(pt)} = \left( -2k_1 \theta' - \frac{4(k_2 - k_1) \theta' (1 - \theta')}{\{1 - 4\theta' (1 - \theta') (1 - e^{\omega/RT})\}^{1/2} + 1} \right) (1 - \theta'), \quad (9)$$

where  $\omega$  is the pair-wise interaction energy in the [001] direction. As in section

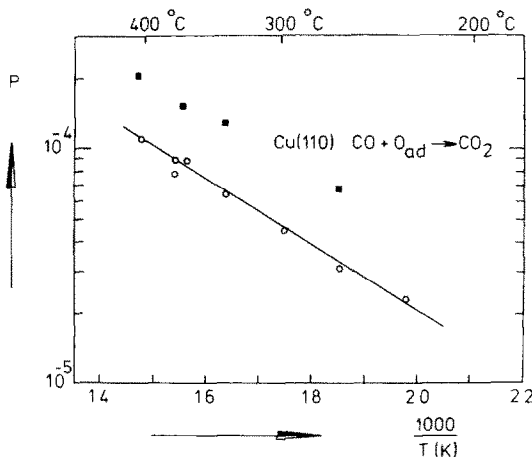


Fig. 9. Arrhenius plot of the reaction probability of CO with  $O_{ad}$  taken at  $\theta = \delta \Delta \approx 0.25$ ; (■) values of  $k_1$ , obtained by fitting the integral of eq. (9) to the measurements of fig. 8.

4.3, the coverages are normalized to  $\theta' = 1$  at half a monolayer of adsorbed oxygen atoms. A non-zero reaction rate is assumed at  $\theta' = 1$ , which is ascribed to a few empty sites, defects or to a reaction with a much lower rate.

There are three parameters  $k_1$ ,  $k_2$  and  $\omega$ , which can be varied so that eq. (9) fits the curves of fig. 8. For  $\omega$  we took 4 kcal/mol, as in fig. 6. The dots in fig. 8 are obtained by numerical integration of eq. (9), with starting point  $\theta = 0.95$  and the values for  $k_1$  and  $k_2$  are as indicated. Good fits are obtained for  $k_2 = 2k_1$ , independent of  $T$ , indicating that the removal of lone oxygen atoms is somewhat more likely than that of row atoms. A possible reason is that a lone oxygen atom has more free nn sites than a row atom.

In fig. 9 the values for the reaction probability  $P$  (defined as the number of removed oxygen atoms per incident CO molecule), calculated in the nearly linear (midway) part of the curves of fig. 8, are depicted in an Arrhenius plot. Also depicted are the values of  $k_1$ , obtained by the fits of eq. (9). In this model the midway reaction probability  $P$  is about equal to  $0.6 k_1$  in the considered temperature range, indicating that the slope of an Arrhenius plot of  $P$  is approximately equal to the activation energy of the reaction, of which  $k_1$  is the rate constant. This is illustrated in fig. 9. The activation energy appears to be  $6.3 \pm 0.3$  kcal/mol, which is in reasonable agreement with the value 5 kcal/mol obtained by Ertl [11]. To this value of 6.3 kcal/mol should be added the heat of adsorption of CO on Cu(110). We thus obtain as the activation energy for the suggested rate-limiting step  $CO_{ad} + O_{ad} \rightarrow CO_2 \uparrow$  a value of 19 kcal/mol, which is equal to that for Cu(111) (18–20 kcal/mol [12]). The absolute values for the overall reaction probabilities also appear to be equal ( $\sim (3-4) \times 10^{-5}$ , 250°C,  $\theta \approx 0.25$ ). Thus this reaction seems rather structure-insensitive.

## 6. Conclusions

(i) In the chemisorption stage the  $\delta\Delta$  and  $\delta\psi$  per adsorbed oxygen atom depend on the temperature, the oxygen coverage and the azimuth of the plane of incidence.

(ii) The initial sticking probability for O<sub>2</sub> is about 0.2. The rate of adsorption is independent of the crystal temperature up to a coverage of half a monolayer. We can describe the process by Langmuir kinetics into which dissociative adsorption on empty nn site pairs and an attractive interaction in the adsorbed layer in the [001] direction are incorporated, as is suggested by the sequence of LEED patterns.

(iii) The initial reaction probability of N<sub>2</sub>O at room temperature is 0.15 and decreases with increasing temperature. The saturation coverage is 0.5 monolayer up to exposures of 10<sup>5</sup> L and temperatures of 400°C. The activation energy increases with the oxygen coverage. The LEED sequence observed was the same as that with O<sub>2</sub>.

(iv) The reaction of CO with preadsorbed oxygen proceeds via a Langmuir–Hinshelwood mechanism with an activation energy for the reaction  $\text{CO}_{\text{ad}} + \text{O}_{\text{ad}} \rightarrow \text{CO}_2$  of about 19 kcal/mol. The overall reaction probability at  $\theta \approx 0.25$  is  $3 \times 10^{-5}$  at 250°C.

## Acknowledgement

The authors thank Dr. O.L.J. Gijzeman for helpful discussions and Mr. A.H.J. Huijbers for technical assistance. The investigations were supported by the Netherlands Foundation of Chemical Research (SON) with financial aid from the Netherlands Organization for the Advancement of Pure Research (ZWO).

## References

- [1] G. Ertl, *Surface Sci.* 6 (1967) 208.
- [2] G.W. Simmons, D.F. Mitchell and K.R. Lawless, *Surface Sci.* 8 (1967) 130.
- [3] N. Takahashi, H. Tomita and S. Motoo, *Compt. Rend. (Paris)* B269 (1969) 618.
- [4] A. Oustry, L. Lafourcade and A. Escaut, *Surface Sci.* 40 (1973) 545.
- [5] G. Ertl and J. Küppers, *Surface Sci.* 24 (1971) 104.
- [6] T.A. Delchar, *Surface Sci.* 27 (1971) 11.
- [7] I.E. Wachs and R.J. Madix, *Appl. Surface Sci.* 1 (1978) 303.
- [8] A.G.J. de Wit, R.P.N. Bronckers and J.M. Fluit, *Surface Sci.* 82 (1979) 177.
- [9] F.W. Young, J.V. Cathcart and A.T. Gwathmey, *Acta Met.* 4 (1956) 145.
- [10] J.J.F. Scholten and J.A. Konvalinka, *Trans. Faraday Soc.* 65 (1969) 2465.
- [11] G. Ertl, *Surface Sci.* 7 (1967) 309.
- [12] F.H.P.M. Habraken, E.Ph. Kieffer and G.A. Bootsma, *Surface Sci.* 83 (1979) 45.
- [13] F.H.P.M. Habraken and G.A. Bootsma, *Ned. Tijdschr. Vacuumtech.* 16 (1978) 142.
- [14] F.H.P.M. Habraken, G.A. Bootsma, P. Hofmann, S. Hachicha and A.M. Bradshaw, to be published.

- [15] J.V. Cathcart, J.E. Epperson and G.F. Petersen, *Acta Met.* 10 (1962) 699.  
J.V. Cathcart and G.F. Petersen, in: *Ellipsometry in the Measurement of Surfaces and Thin Films*, Eds. E. Passaglia, R.R. Stromberg and J. Kruger (Natl. Bur. Std. Misc. Publ. 256, US Govt. Printing Office, Washington, DC, 1964) p. 201.
- [16] F.H.P.M. Habraken, O.L.J. Gijzeman and G.A. Bootsma, to be published.
- [17] P. Hofmann, R. Unwin, W. Wyrobisch and A.M. Bradshaw, *Surface Sci.* 72 (1978) 635.
- [18] H. Albers, W.J.J. van der Wal, O.L.J. Gijzeman and G.A. Bootsma, *Surface Sci.* 77 (1978) 1.
- [19] C. Benndorf, B. Egert, G. Keller, H. Seidel and F. Thieme, *J. Vacuum Sci. Technol.* 15 (1978) 1806.
- [20] T.L. Hill, *Introduction to Statistical Thermodynamics* (Addison-Wesley, London, 1962) ch. 14.
- [21] D.A. King and M.G. Wells, *Proc. Roy. Soc. (London)* A339 (1974) 245.
- [22] A.G.J. de Wit, Thesis, Univ. of Utrecht (1979).
- [23] J.H. Lunsford, *Catalysis Rev.* 8 (1973) 135.
- [24] S.G. Gagarin and Yu.A. Kolbanovskii, *Kinetics and Catalysis* 18 (1977) 744.
- [25] P.O. Gartland, S. Berge and B.J. Slagsvold, *Phys. Rev. Letters* 28 (1972) 738.
- [26] H.A. Engelhardt, A.M. Bradshaw and D. Menzel, *Surface Sci.* 40 (1973) 410.
- [27] H.A. Engelhardt and D. Menzel, *Surface Sci.* 57 (1976) 591.
- [28] T. Engel and G. Ertl, *J. Chem. Phys.* 69 (1978) 1267.
- [29] T. Matsushima, *Surface Sci.* 79 (1979) 63.
- [30] K. Horn, M. Hussain and J. Pritchard, *Surface Sci.* 63 (1977) 244.